Simulation analysis of climate suitability of radiation cooling technology in residential buildings

Abstract: Long-wave radiation cooling is an effective method for designing the thermal environment of buildings. Different climate regions use the steady-state calculation method of the surface heat transfer coefficient, which can cause a significant deviation between the heat exchange of the protective structure and the building cooling design. To evaluate the influence of climate environment and surface emissivity on building heat transfer in summer, the IESVE numerical simulation method was used to calculate the summer long-wave radiation of 9 typical residential buildings in different climate regions. The results show that the building can effectively radiate heat through sky radiation when the outdoor relative humidity is lower than 60% and the temperature difference in summer is greater than 12°C. The effect of sky radiation is significantly affected by climate. The difference in summer radiation of buildings in different regions reaches 1687 kW. The sky radiation influence rate in Beijing and Xi'an reaches 38.4% and 32.2%. Long-wave radiation cooling can reduce the natural heat gain of buildings in summer by one-third. When the surface emissivity increases from 0.3 to 0.9, the proportion of building heat transfer varies from 1.5% to 13.8%.

Keywords: long-wave radiation cooling; numerical simulation; building load; surface emissivity; climate adaptability

Highlights：

This study utilized CDD26 as the representative climate zone to simulate the long-wave radiation of multi-story residential buildings for the first time.

The research evaluated the impact of changes in surface emissivity (ranging from 0.3 to 0.9) on building heat exchange.

The study assessed the applicable meteorological conditions and the distribution of application ranges for sky radiation technology.

1. Introduction

Buildings account for 20% to 40% of global fossil energy consumption. With the rapid development of urbanization, the average energy intensity of urban residential households continues to increase.[V. Gupta,2023.] In recent years, as the thermal insulation level of building envelopes has been steadily improving, the discussion on building envelope energy conservation has focused on how to control natural heat dissipation in buildings and the resulting increase in air-conditioning energy consumption [Hideyo Nimiya,2022]. Sky radiant cooling technology can enhance the building's heat dissipation efficiency without the need for additional energy sources, showing promising potential for building energy savings.

The Earth receives its energy from the sun and emits an equal amount of energy as thermal radiation to maintain global thermal balance.[Dnyandip K,2019] The temperature of outer space beyond the atmosphere is close to absolute zero, serving as an ideal cold source.Terrestrial surfaces exposed to sunlight absorb solar heat and shed heat back to outer space as infrared radiation. If the radiated heat is greater than the solar energy absorbed, then daytime radiative cooling is achieved passively, without any energy input. However, the atmosphere hinders

ground objects from directly radiating heat into space. As a translucent medium, the atmosphere possesses dynamic properties of absorbing, scattering, and emitting radiation, allowing the passage of infrared radiation in a specific wavelength range without absorption. Inverse radiation significantly relies on the wavelength. Within the 8 ~ 13 μ m band, the absorption rate of carbon dioxide and water vapor in the atmosphere is minimal, enabling substantial penetration. This band falls within the far-infrared region of the ground object itself, commonly referred to as the far-infrared window of the atmosphere. Radiant sky cooling leverages the sky as a heat sink, dissipating building heat to the sky through far-infrared windows [Qiliang Wang,2024]. Chenxi Sui, et al.develop an aqueous flexible electrochromic design for use as a building envelop based on graphene ultra-wideband transparent conductive electrode and reversible copper electrodeposition, in which the thermal emissivity can be tailored to vary between 0.07 and 0.92 with excellent long-term durability.[Chenxi Sui,2023]Building energy simulations show that building envelopes can save on year-round operational HVAC energy consumption across the United States by up to 43.1 MBtu on average in specific zones.

List of symbols

A	area (m_2)	S_h	hourly insolation rate
C	heat capacity rate (J/K)	N_h	hourly cloud cover
h	Planck's constant (J·s)	P_g	the ground short-wave albedo
h_c	heat transfer coefficient ($W/(m^2 \cdot K)$)	G_h	hourly solar radiation ($W \cdot h/m^2$)
$I_{AM1.5}$	solar illumination (W/m^3)	ε	emissivity
I_{BB}	spectral radiance of a blackbody ($W/(sr \cdot m^3)$)	θ	angle (°)
k	thermal conductivity (W/(m·K))	λ	wavelength (m)
k_B	Boltzmann constant (J/K)	τ	transmittance
N	number	Ω	solid angle (sr)
P	power (W)	σ	Stephen Boltzmann constant (W/m2·K4)
q	heat (W)		
q_{gen}	internal heat generated (W)	*Subscripts*	
R	thermal resistance (K/W)		
T	temperature (K)	air	Air
ΔT_{LM}	logarithmic mean temperature difference (LMTD) (K)	atm	Atmosphere
		cool	Cooling
V	velocity (m/s)	con	parasitic heat gain
F	long-wave radiation flux	prc	passive radiative cooler
T_{eo}	Absolute surface temperature (K)	r	Room
T_a	the absolute air temperature (K)	rad	Radiation
σ_W	the partial pressure of water vapor (hPa)	sun	solar radiation
		β	surface Inclination (°)

For a thorough evaluation of buildings' long-wave radiation cooling potential under diverse climatic conditions, it is necessary to comprehend long-wave radiation cooling technology and its application performance parameters comprehensively. The application of sky radiation cooling technology is constrained by various factors, primarily including climatic conditions, building environment spatial constraints, and building envelope surface material radiation performance.

In the realm of model development and climate potential prediction, Yucan Peng et al. designed colored low-emissivity films based on the solar spectrum and thermal radiation spectrum. They developed a thermal model to quantify the reduction of heat gain and loss through a wall by applying these films. The study focused on the exterior walls of a post-1980 midrise apartment building as defined by the US Department of Energy. The researchers calculated the average effect of heat transmission reduction per unit area of the installed wall.[Yucan Peng,2021].Panchabikesan assessed the monthly and annual average cooling potential in different climate zones like India. The annual average passive cooling potential in hot and dry climates could reach up to 251W/m2, while warm and humid climate zones had an average of 127W/m2 [Karthik Panchabikesan,2017]. T. S. Eriksson's atmospheric model study revealed that changes in water vapor content exert a more significant influence on radiative cooling compared to changes in ozone and aerosols [T. S. Eriksson,1982].

Extensive theoretical research has been conducted on long-wave radiation cooling materials in the building energy-saving sector, covering the classification, working principles, application status, and future trends of long-wave radiation cooling technology. Cooling performance in parameter influence analysis is contingent on material properties such as thermal surface emissivity and reflectivity, alongside the surface's environmental level.

Notable climate discrepancies exist across various regions of the country, leading to divergent application potentials of long-wave radiation cooling technology. Nonetheless, the standard calculation in building thermal design codes overlooks long-wave radiation's impact, particularly the influence of sky radiative cooling on building heat transfer remains relatively unexplored. This paper's first chapter analyzes the selection of the sky radiation model, the second chapter sets calculation conditions, the third chapter calculates buildings' long-wave radiation in different climate zones, and statistically analyzes suitable climatic parameters for long-wave radiation cooling technology. The fourth chapter conducts sensitivity analysis on the influence of surface material emissivity on building heat transfer in diverse climatic regions. The fifth chapter summarizes the classification, working principles, application status, and future trends of long-wave radiation cooling technology. Through an examination of applicable climatic conditions and material properties of sky radiation cooling technology, this study holds practical value for the technology's application.

2. Methodology

Firstly, under the comprehensive review of computational models, we have selected simulation models for our experimental calculations, and the specific details will be described in the following text. These models are similar in terms of radiation performance, with the main difference lying in their model accuracy. Based on hourly meteorological parameters from typical year meteorological data, we can analyze the heat load of residential buildings in each city (Step 1). This involves the use of representative multi-story residential building physical models to compare climate differences under conditions of no geometric shape differences. Building energy consumption simulations are used in the following steps. Step 2 involves classifying and zoning each representative climate, and graphically representing the zoning results with overall radiation potential. Finally, a sensitivity analysis of radiation rates is conducted for each representative city, and the numerical radiation results are compared with the overall heat gain.

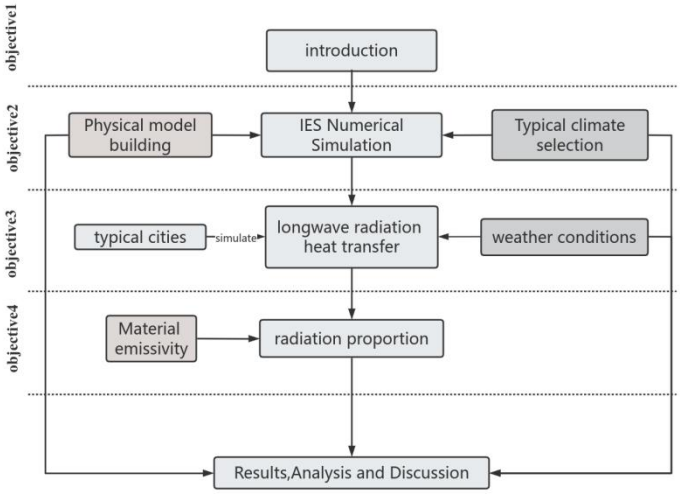

Figure 1. Technology Roadmap.

2.1. Calculation of long-wave radiation

In the process of surface heat balance of the envelope structure, the heat gained by the wall is equal to the absorbed solar radiation heat minus the surface convective heat transfer, and then minus the radiative heat exchange with the ground and the long-wave radiation heat exchange with the atmosphere [Jianheng Chen,2020]. The essence of long-wave radiation is the radiation heat exchange between buildings and the sky, including the heat exchange between the ground and the surrounding building environment. The long-wave absorption rate is equal to the long-wave emissivity ε_1, and the calculation is complicated, and the total absorption flux is the absorbed atmospheric component $\varepsilon_1 L_{sky(\beta)}$ and the absorbed ground component $\varepsilon_1 L_{g(\beta)}$.

$$F = \varepsilon_1 \sigma T_{eo}^4 \quad (1)$$

where F is the long-wave radiation flux emitted by the surface (W·m-2); ε_1 is the long-wave surface emissivity; σ is the Stephen Boltzmann constant (5.6697 × 10-8) (W·m-2·K -4); T_{eo} is Absolute surface temperature (K).

The output long-wave flux is independent of the orientation of the emitting surface. The resulting slanted long-wave radiation energy exchange can be expressed as a net balance. The expression for the net long-wave radiation entering the surface of the envelope:

$$L(\beta) = \varepsilon_1 \left[F_{s-sky} L_{sky(\beta)} + F_{s-g} L_{g(\beta)} - \sigma T_{eo}^4 \right] \quad (2)$$

where $L(\beta)$ is the long-wave radiation exchange (W · m-2); $L_{sky(\beta)}$ is the atmospheric long-wave radiation received directly from the sky (W·m-2); $L_{g(\beta)}$ is the long-wave radiation received from the ground (W·m-2); β is the surface Inclination (°); F_{s-g} is the angle coefficient of the outer surface facing the ground; F_{s-sky} is the angle coefficient of the outer surface facing the sky.

$$F_{s-g} = (1-\cos\alpha)/\ \alpha \quad (3)$$

$$F_{s-sky} = (1-\cos\alpha)/\ \alpha \quad (4)$$

For the special case of no occlusion on the horizontal plane, equation 2 is simplified to:

$$L = \varepsilon_1 \left(L_{sky} - \sigma T_{eo}^4 \right) \quad (5)$$

2.2. Sky Radiation Model

Various formulas have been proposed to estimate the long-wave radiation emitted from the atmosphere downwards and the ground upwards. Some models have been developed [Luca Evangelisti,2019] for calculating the effective sky temperature on the horizontal plane under clear sky conditions. The general empirical value was to subtract 6K from the outdoor air temperature, which was the horizontal effective sky temperature [Angélica Walsh,2019]. The procedure used here was based on the Correlations of the sky effective emissivity in atmosphere window [Tian Yan,2024], and these detailed models formed the basis for the numerical simulation of long-wave radiation calculations. The daytime long-wave irradiance of the atmosphere on the horizontal plane can be estimated as:

$$L_{sky} = \sigma T_a^4[0.904 - (0.304 - 0.061\rho w^{1/2})S_h - 0.005\rho w^{1/2}] \quad (6)$$

where L_{sky} is the daytime long-wave irradiance (W · m-2) on the horizontal plane; σ is the Stephen Boltzmann constant (5.6697 × 10 – 8) (W · m-2 · K -4); T_a is the absolute air temperature (K); ρw is the partial pressure of water vapor (hPa), and S_h is the hourly insolation rate.

At night, S_h is replaced with $[1 - (N_h/8)]$, where N_h is hourly cloud cover. Since the values of S_h are not stable during the first and last hours of the day, these two hours are considered nighttime hours. The daytime terrestrial long-wave upward flux is:

$$L_g = \sigma\left[0.980T_a + 0.037(1 - \rho_g)G_h\right]^4 \quad (7)$$

where L_g is the long-wave radiation flux (W·m-2) on the horizontal plane; T_a is the absolute air temperature (K); ρ_g is the ground short-wave albedo, and G_h is the hourly solar radiation (W·h·m-2).

3. Case study

3.1 Selection of typical cities

The air conditioning degree-days (CDD26), an indicator that represents the duration and intensity of heat in a region, were used as the standard and divided into three categories based on cooling demand. Representative cities and climate zones were selected[Junwei Liu,2020] as indicated in Table 1 . The hottest period, from May 26th to September 22nd, as shown in Table 2, was identified as the summer research period, with a relatively concentrated cooling period from June 25th to August 25th.

Table 1. Refrigeration requirement classification.

Cooling level	Representative city	CDD26（℃·d）	Thermal partition
	Turpan	579	Cold regions
level 1	East	530	Hot summer and warm winter area
	Haikou	427	Hot summer and warm winter area
	Guangzhou	313	Hot summer and cold winter area
level 2	Wuhan	283	Hot summer and cold winter area
	Chongqing	217	Hot summer and cold winter area
	Karamay	196	Frigid regions
level 3	Xi'an	153	Cold regions
	Beijing	94	Cold regions

Table 2. Typical city air conditioning period in various climate regions.

Climate zone	Typical city	Air conditioning period
Frigid regions	Harbin	None
Cold regions	Beijing	June 20 to August 3

Hot summer and cold winter area	Changsha	June 25 to August 23
Hot summer and warm winter area	Guangzhou	May 26 to September 22
Temperate area	Kunming	None

3.2 Simulation Settings

A typical multi-storey residential building, as shown in Figure 2, with dimensions of 15m×15m×18m and a surface area of 1305 ㎡, is selected as the subject for calculation[Sarah Truchet,2024&Yingchun Ji,2019]. The calculations and simulations are conducted using IESVE numerical simulation software, specifically ApacheSim, ApacheHVAC, MacroFlo, ApacheCalc, and ASHRAE loads. Standard CSWD weather files are used for outdoor boundary conditions. The building structure properties are detailed in Table 3. The indoor calculation temperature is set at 26° C, with a ventilation rate of 0.6/h. The envelope structure has a long-wave emissivity of 0.9 and a surface absorption rate of 0.7. The ground reflectivity is 0.2. A time step of 6 minutes is utilized in Apache sim, with a preprocessing period of 10 days.

Table 3. Physical parameters of envelope.

Name	Structure level (from outside to inside) (mm)	Thermal Conductivity
Exterior wall	10 thick facing brick; 30 thick EPS board; 100 thick reinforced concrete; 10 thick gypsum board	0.58
Roof	10 thick stone panels; 5 thick asphalt layers; 150 thick cast concrete; 80 thick fiberglass mats; 100 thick hollow blocks; 10 thick ceiling slabs	0.38
Ground	25 thick laminated board; 60 thick foam polystyrene insulation board; 100 thick reinforced concrete; 250 thick facing brick; 750 thick clay;	0.24
Floor	60 mm paving tiles; 120 mm concrete floor slabs	2.80
External window (with frame)	Low-e hollow double window	2.16
Exterior doors	Wooden door	2.19
Partition	13 thick cement mortar; 105 thick non-load-bearing hollow brick; 13 thick cement mortar	1.69

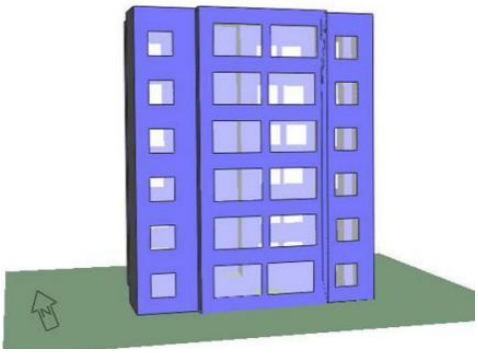

a. Physical model

Figure 2. Simulated physical model.

4. Results and discussion

4.1. Building long-wave radiation

The calculation of total summer long-wave radiation of a building in different climatic regions

includes consideration of the long-wave radiation difference between the horizontal roof and the atmosphere, as well as the long-wave radiation exchange between the vertical surface of the envelope and the surrounding environment. The building is assumed to be in an ideal environment where long-wave radiation and long-wave reflection from surrounding buildings are ignored. The calculation is done using formula (2) and depicted in Figure 3.

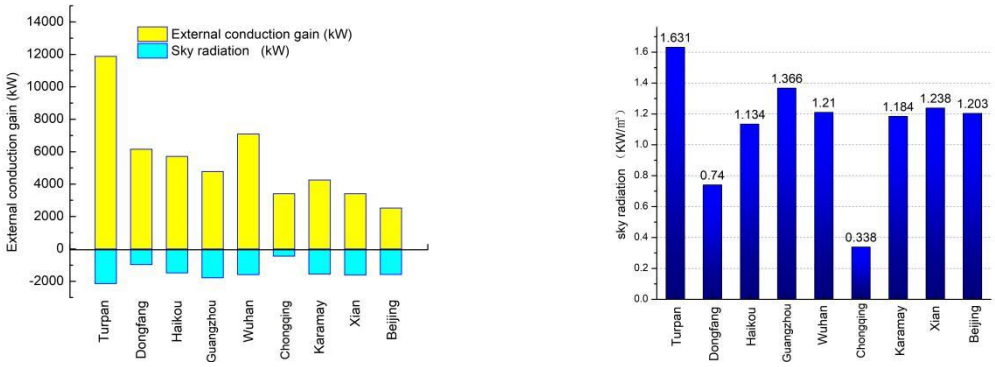

(a) Influence rate of long wave radiation of the envelope in summer

(b) Influence rate of long wave radiation of the envelope in summer

Figure 3. Long-wave radiation values in summer in each city.

The total summer long-wave radiation in each city ranges from 442 to 2129 KW, and the cooling of summer long-wave radiation is significantly influenced by the climate. Among them, Turpan experiences the highest summer long-wave radiation at 2129 KW, while most cities have long-wave radiation levels concentrated in the range of 1479-1782 KW. The cooling effect of long-wave radiation is notably lower in certain regions, with total values in summer being 442 KW and 966 KW respectively. There is no linear relationship between the change in long-wave radiation in each city and the number of air-conditioning degree-days. Except for the relatively stable radiation value in the 3-level area, there is a significant difference in the radiation amount among the selected cities in the 1st and 2nd levels. The application of long-wave radiation cooling technology is influenced by specific heating factors in each region, and the comprehensive evaluation of its applicability should consider the relationship between key meteorological factors and building heat dissipation in each region.

4.2. Influence of long-wave radiation heat transfer

The calculation of heat gain in the building's outer envelope is essential for determining the building load and designing the thermal properties of the envelope. It involves a complex process of accounting for solar radiation heat gain, heat transfer due to indoor and outdoor temperature differences, and dissipation of long-wave radiation heat. In building thermal design, simplified outdoor boundary conditions are used for long-wave radiation calculations. A value of 3.5℃ is used for the roof and 1.8℃ for the outer wall (Evangelisti, 2022). To assess the impact of long-wave radiation on summer heat gain in building envelopes across different climates, the heat gain influence rate is calculated for buildings in each city.

$$P = \frac{q_l}{q_h + q_l} \cdot 100\% \quad (8)$$

where P is the influence rate of long-wave radiation on building heat gain; ql is long-wave radiation heat dissipation, kw; qh is the heat gain of the building envelope, kw. Figure 4 shows the heat gain and impact rate of the urban envelope structure.

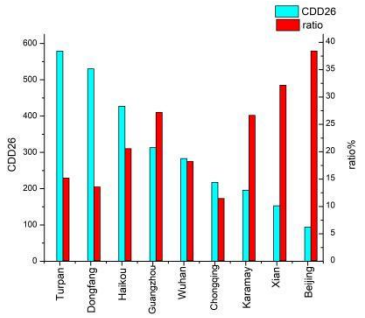

Figure 4. Sky radiation cooling ratio.

Figure 4 shows that the range of variation in the long-wave radiation impact rate is between 11.4% and 38.4%, with different trends compared to the total long-wave radiation value. The influence of long-wave radiation performance and building heat gain is higher in Beijing and Xi'an, reaching 38.4% and 32.2%, respectively. In these areas, only one-third of the building's natural heat gain in summer can be reduced through long-wave radiation cooling. Chongqing and the eastern region have the lowest heat gain rates at 11.5% and 13.6%, respectively, due to low total long-wave radiation values. Despite Turpan having a much higher total long-wave radiation compared to other regions, the impact rate is only 15.2%. This is because buildings in Turpan receive significant natural heat, and building heat-proof design should consider factors such as building shading, reflected radiation, and long-wave radiation in this area. When designing building heat protection, the impact of long-wave radiation can be assessed based on the building's heat gain influence rate in different climatic regions, and outdoor calculation boundaries can be adjusted for areas with high impact rates.

4.3. Applicable weather conditions

Formula (6-7) indicates that the effective sky temperature and ground radiation undergo dynamic changes due to various factors such as absolute air temperature, water vapor partial pressure, hourly insolation rate, and ground albedo. With numerous influencing parameters and a complex calculation process, it is challenging to determine the applicability of long-wave radiation technology. Typically, dry bulb temperature, relative humidity, and solar radiation are used as the primary meteorological indicators for building load and thermal design in outdoor building design. Therefore, based on the analysis of long-wave radiation cooling calculations, the Turpan area is considered a high-efficiency zone for long-wave radiation cooling technology application (ZONE I), while Chongqing and the eastern region are classified as low-efficiency zones (ZONE III), with other areas falling under general application zones (ZONE II). By comparing the key meteorological characteristics of these zones, the applicable climate range for sky radiation cooling technology is calculated, as shown in Figure 5-7.

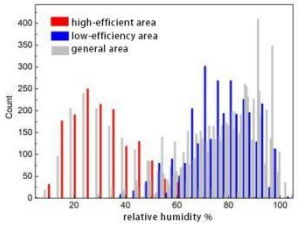

Figure 5. Frequency distribution of hourly relative humidity in summer

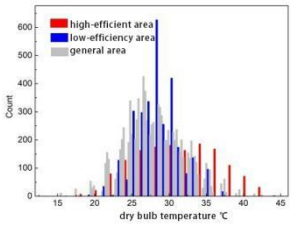

Figure 6. Frequency distribution of hourly dry bulb temperature in summer

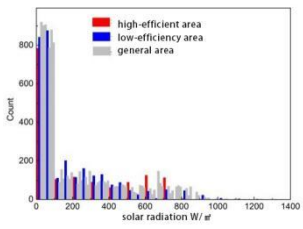

Figure 7. Distribution of hourly solar radiation frequency in summer

It is evident from Figure 5 that the application discrepancy caused by the relative humidity index is significant. ZONE I has a relative humidity range of 10% to 60%, while ZONE II shows poor heat dissipation effects at 40% to 100%. Lower relative humidity in summer is more conducive to long-wave radiation cooling.

The maximum temperature in ZONE I exceeds 35℃, while ZONE II does not show significant characteristics. The characteristic dry bulb temperature in ZONE III is mainly concentrated between 25-30℃, with a frequency of over 200 hours. A higher mean absolute deviation of the dry bulb temperature promotes radiative cooling from the sky. This is consistent with the findings of Yazhu Zhu (2021), which suggest that a greater temperature difference corresponds to a higher potential for radiative cooling from the sky.

Solar radiation in ZONE I is evenly distributed, with no distinct characteristics in ZONE II. The frequency of characteristic solar radiation in ZONE III decreases within the range of 200-600 W/㎡, with a frequency difference of less than 100 between zones. Therefore, utilizing solar radiation as an evaluation index for sky radiation potential is not effective.

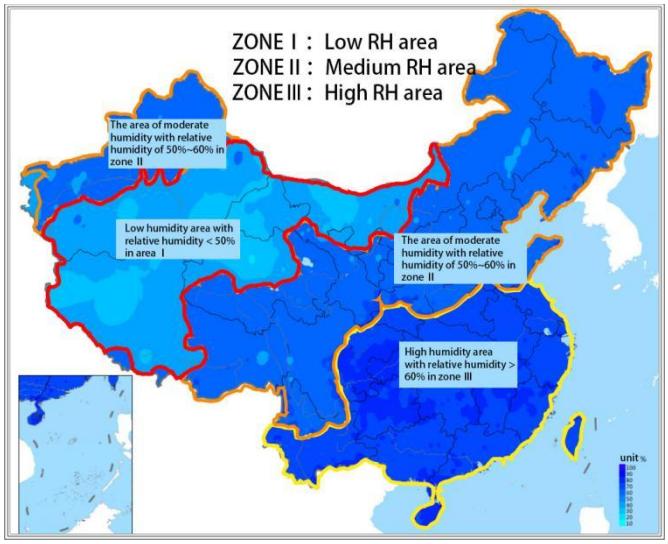

Figure 8. Scope of application diagram.

4.4 Analysis of Sensitivity to Long-wave Radiation Emissivity

In engineering, the temperature of objects involved in radiative heat transfer is mostly below 2000 K. Actual objects can be approximately regarded as gray bodies within the infrared wavelength range. For most engineering materials, changes in radiative properties in different directions are not considered, and it is believed that the approximation of obeying Lambert's law can simplify the calculation of actual radiative heat transfer through (Equation 1). The long-wave radiation range of commonly used building materials is within 0.18 to 0.98. Materials with surface emissivities of 0.3, 0.5, 0.7, and 0.9 are selected for building load simulation calculations under different climates. The potential of surface emissivity is compared based on the proportion of the load caused by long-wave radiation, as shown in Figure 8. The calculation results are presented in Table 4.

Table 4 Comparison of summer building loads in various cities

city	Load /kw	Radiation emissivity 0.3	0.5	0.7	0.9	city	Load /kw	Radiation emissivity 0.3	0.5	0.7	0.9
Turp	Cooling	350	342	336	330	Chon	Cooling	131	131	131	131

an	load	04	24	00	89	gqing	load	80	71	62	53
	long-wave radiation	1205	1578	1879	2126		long-wave radiation	203	271	337	402
	Proportion	3.4%	4.6%	5.6%	6.4%		Proportion	1.5%	2.1%	2.6%	3.1%
	Cooling load	20150	20008	19881	19767		Cooling load	16713	16478	16272	16091
Dongfang	long-wave radiation	516	683	832	965	Karamay	long-wave radiation	792	1044	1263	1455
	Proportion	2.6%	3.4%	4.2%	4.9%		Proportion	4.7%	6.3%	7.8%	9.0%
	Cooling load	19500	19158	18867	18615		Cooling load	14314	13955	13651	13391
Haikou	long-wave radiation	819	1075	1289	1470	Xi'an	long-wave radiation	845	1106	1321	1502
	Proportion	4.2%	5.6%	6.8%	7.9%		Proportion	5.9%	7.9%	9.7%	11.2%
	Cooling load	17382	16990	16665	16391		Cooling load	11784	11405	11084	10807
Guangzhou	long-wave radiation	993	1297	1547	1755	Beijing	long-wave radiation	841	1100	1314	1494
	Proportion	5.7%	7.6%	9.3%	10.7%		Proportion	7.1%	9.6%	11.9%	13.8%
Wuhan	Cooling load	22135	21678	21298	20978						
	long-wave radiation	852	1116	1330	1507						
	Proportion	3.8%	5.1%	6.2%	7.2%						

As can be seen from Table 4, the calculated results of building loads are basically consistent with the cooling classification. Level 1 is significantly higher than other regions, with the highest reaching 35004KW in Turpan. When the emissivity increases from 0.3 to 0.9, the building load decreases by 1915KW. The highest building loads in Dongfang and Haikou are 20150KW and 19850KW, respectively, and the loads decrease by 383KW and 885KW respectively when the emissivity increases. Among the Level 2 regions, Guangzhou has the highest summer load of 17382KW, and Wuhan is higher than some Level 1 regions, reaching a maximum of 22135KW. The loads decrease by 991KW and 1157KW respectively. Chongqing has a load of 13180KW, with only a decrease of 27KW. In Level 3 regions, Beijing's summer load is significantly lower than other regions, at 11784KW, but the load decreases by 977KW during the increase of emissivity, which is higher than Xi'an and Karamay.

The long-wave radiation load proportion exhibits a consistent trend of increasing with the increase in radiative emissivity across all cities, but the magnitude of change varies. The effective regions of long-wave radiation are significantly higher than the ineffective regions. The range of change in the proportion of building loads among the selected cities is 1.5~13.8%, with higher proportions in Beijing, Xi'an, and Guangzhou, specifically 7.1~13.8%, 5.9~11.2%, and 5.7~10.7%, respectively. When the emissivity increases from 0.3 to 0.9, the highest increase in load proportion is 6.7%. The load proportions in Karamay, Haikou, Wuhan, and Turpan increase by 4.3%, 3.7%, 3.3%, and 3.0%, respectively. Chongqing and Dongfang have load proportions below 4.8%, with similarly low growth rates. Selecting materials with higher emissivity for the envelope surface is more conducive to reducing the summer building load. The method of increasing long-wave radiative heat dissipation by altering the surface emissivity is more significant in effective regions of long-wave radiation.

5. Conclusion

Climate differences have a significant impact on the cooling effect of long-wave radiation. In the nine selected cities, the range of long-wave radiation in summer varies from 442 to 2129KW. With the exception of a few cities, most have a similar range of 1479 to 1782KW. The Turpan area stands out with a notably higher long-wave radiation value of 2129KW, while the East and Chongqing areas have relatively lower values of 966KW and 442KW, respectively.

A long-wave radiation cooling design method based on climate classification is proposed, utilizing outdoor relative humidity, dry bulb temperature, and sky effective temperature as indicators for climate classification. Statistical analysis of hourly frequency reveals that the optimal climate for long-wave radiation cooling technology is characterized by a relative humidity below 60% and an outdoor temperature difference exceeding 12℃.

Implementation of long-wave radiation cooling technology can reduce the heat gain of building envelopes in the selected areas. Beijing and Xi'an are particularly suitable, achieving reductions of 38.4% and 32.2% in natural heat gain during summer. In practice, passive heat gain paths of building structures should be considered, with technologies such as shading and reflected radiation utilized to enhance the effectiveness of long-wave radiation cooling technology.

By increasing the surface emissivity of envelope structures, the cooling load of buildings can be reduced. Turpan experiences the largest drop in cooling load at 1915KW, while Chongqing and Dongfang see the smallest drops at 27KW and 383KW. The proportion of long-wave radiation load increases by 5.0% to 6.7% in Beijing, Xi'an, and Guangzhou, but only by 2.3% and 1.5% in the East and Chongqing. In other regions, changing the surface material emissivity can increase the

proportion of long-wave radiation load by at least 3.0%.

Disclosure statement

No potential conflict of interest was reported by the authors.

Notes on contributors

Professor Fan Yue is engaged in the improvement of residential building quality and performance-based renovation design; Dr. Chen Jie is involved in the thermal design and climate adaptability research of green buildings;

Funding:

This study was supported by the NSFC of China General Program (NO.52178020) and Guangdong Basic and Applied Basic Research Foundation Natural Science Foundation General Program (NO.2024A1515010891);Guangdong Basic and Applied Basic Research Foundation Joint Fund Youth Project (NO.2023A1515110736).

Data availability statement:

All data included in this study are available upon request by contact with the corresponding author.

References

[1]V. Gupta,C. Deb. Envelope design for low-energy buildings in the tropics: A review[J]. Renewable and Sustainable Energy Reviews, 2023, 186: 113650.

[2]I Dewa Gede Arya Putra,Hideyo Nimiya,Ardhasena Sopaheluwakan, et al. Development of climate zones for passive cooling techniques in the hot and humid climate of Indonesia[J]. Building and Environment, 2022, 226: 109698.

[3]Dnyandip K. Bhamare,Manish K. Rathod,Jyotirmay Banerjee. Passive cooling techniques for building and their applicability in different climatic zones — The state of art[J]. Energy and Buildings, 2019, 198: 467-490.

[4]Qiliang Wang,Ya Dan,Saffa Riffat, et al. Harvesting energy from the sun and space: A versatile collector for simultaneous production of electricity, heat, and cold energy[J]. The Innovation Energy, 2024, 1(1): 100013.

[5]Chenxi Sui,Jiankun Pu,Ting-Hsuan Chen, et al. Dynamic electrochromism for all-season radiative thermoregulation[J]. Nature Sustainability, 2023, 6(4): 428-437.

[6]Yucan Peng,Lingling Fan,Weiliang Jin, et al. Coloured low-emissivity films for building envelopes for year-round energy savings[J]. Nature Sustainability, 2021, 5: 339-347.

[7]Karthik Panchabikesan,Kumaresan Vellaisamy,Velraj Ramalingam. Passive cooling potential in buildings under various climatic conditions in India[J]. Renewable and Sustainable Energy Reviews, 2017, 78: 1236-1252.

[8]T. S. Eriksson,C. G. Granqvist. Radiative cooling computed for model atmospheres[J]. Applied Optics, 1982, 21(23): 4381.

[9]Jianheng Chen,Lin Lu. Development of radiative cooling and its integration with buildings: A comprehensive review[J]. Solar Energy, 2020, 212: 125-151.

[10]Luca Evangelisti,Claudia Guattari,Francesco Asdrubali. On the sky temperature models and their influence on buildings energy performance: A critical review[J]. Energy and Buildings, 2019,

183: 607-625.
[11]Angélica Walsh,Daniel Cóstola,Lucila Chebel Labaki. Validation of the climatic zoning defined by ASHRAE standard 169-2013[J]. Energy Policy, 2019, 135: 111016.
[12]Tian Yan,Dawei Xu,Jing Meng, et al. A review of radiative sky cooling technology and its application in building systems[J]. Renewable Energy, 2024, 220: 119599.
[13]Junwei Liu,Zhihua Zhou,Debao Zhang, et al. Field investigation and performance evaluation of sub-ambient radiative cooling in low latitude seaside[J]. Renewable Energy, 2020, 155: 90-99.
[14]Junwei Liu,Debao Zhang,Shifei Jiao, et al. Preliminary study of radiative cooling in cooling season of the humid coastal area[J]. Solar Energy Materials and Solar Cells, 2020, 208: 110412.
[15]Sarah Truchet,Arnaud Jay,Etienne Wurtz, et al. Impact of thermal inertia coupled to natural night ventilation. A case study for a high performance building in continental climate[J]. International Journal of Ventilation, 2024, 23(1): 25-38.
[16]Yingchun Ji,Angela Lee,Will Swan. Building dynamic thermal model calibration using the Energy House facility at Salford[J]. Energy and Buildings, 2019, 191: 224-234.
[17]Luca Evangelisti,Roberto De Lieto Vollaro,Francesco Asdrubali. On the equivalent thermo-physical properties for modeling building walls with unknown stratigraphy[J]. Energy, 2022, 238: 121679.
[18]Yazhu Zhu,Hua Qian,Ronggui Yang, et al. Radiative sky cooling potential maps of China based on atmospheric spectral emissivity[J]. Solar Energy, 2021, 218: 195-210.